Characterizing the Charge Trapping across Crystalline and Amorphous Si/SiO2/HfO2 Stacks from First-Principle Calculations

Yue-Yang Liu, Feilong Liu, Runsheng Wang, Jun-Wei Luo, Xiangwei Jiang, Ru Huang, Shu-Shen Li, and Lin-Wang Wang

Phys. Rev. Applied **12**, 064012 — Published 5 December 2019

DOI: 10.1103/PhysRevApplied.12.064012

Characterizing the charge trapping across crystalline and amorphous $Si/SiO_2/HfO_2$ stacks from first principle calculations

Yue-Yang Liu[1,2], Feilong Liu[1], Runsheng Wang[3†], Jun-Wei Luo[1§], Xiangwei Jiang[1*], Ru Huang[3], Shu-Shen Li[1] and Lin-Wang Wang[2‡]

[1]State Key Laboratory of Superlattices and Microstructures, Institute of Semiconductors, Chinese Academy of Sciences, Beijing 100083, China.
[2]Joint Center for Artificial Photosynthesis and Materials Science Division, Lawrence Berkeley National Laboratory, Berkeley, California 94720, USA.
[3]Institute of Microelectronics, Peking University, Beijing 100871, China.

Abstract

The complexity of charge trapping in novel semiconductor devices such as high-k MOSFETs is increasing as the devices themselves become more complicated. To facilitate the research on such charge trapping issues, here we propose an optimized simulation framework that is composed of density functional theory (DFT) for electronic structure calculation and Marcus theory for charge trapping rates calculation. The DFT simulations are either carried out or corrected by HSE hybrid functional. Using this framework, the hole trapping characteristics along multiple paths in $Si/SiO_2/HfO_2$ stacks are investigated, and the relative importance of each path is revealed by calculating its exact hole trapping rate. Besides the study on crystalline stacks, we also create an amorphous stack, which is more realistic compared to experiments and real devices, to reveal more active trapping centers and to study the statistical feature of charge trapping induced by structural disorder. In addition, to seek effective measures for relieving these charge trapping problems, the effects of hydrogen (H) and fluorine (F) passivations are discussed, and physical insights for improving the performance of high-k MOSFETs are provided.

Corresponding authors: *xwjiang@semi.ac.cn; †r.wang@pku.edu.cn; §jwluo@semi.ac.cn; ‡

lwwang@lbl.gov

I. INTRODUCTION

Charge trapping from semiconductors to the coated oxide/nitride/high-k layers is a very important quantum mechanical process in semiconductor physics and applications. On the one hand, charge trapping can be utilized to store information in semiconductor-oxide-nitride-oxide-semiconductor (SONOS) capacitor structures to form non-volatile memory devices [1,2]. On the other hand, charge trapping is a severe problem that needs to be solved to improve the reliability of MOSFETs [3,4], especially high-k MOSFETs, which replace the conventional SiO_2/SiO_xN_y gate dielectrics with high-k materials to reduce gate leakage currents during continuous size scaling [5-7]. Desirable in one case and problematic in the other case, the charge trapping is definitely a key physical process that must be well understood in order to control it in different situations. However, in both cases, as shown schematically in Fig.1, the charge trapping process can happen across multiple interfaces, such as Si/SiO_2, SiO_2/Si_3N_4, and SiO_2/HfO_2 interfaces, which makes the physics complicated and difficult to comprehend, especially if one tries to find out the results merely from fitting to experimental device performance. It will thus be very useful if the problem can be studied by first principle calculations, and different cases can be classified according to their distinct physical behaviors.

The charge trapping phenomenon in MOSFETs is a general process in which carriers in the semiconductor channel are transferred into the gate dielectrics by crossing single or multiple interfaces, and finally trapped in the defective or intrinsic trapping centers in the dielectric oxides. Static defect properties related to the charge trapping process have been investigated widely by using first principles calculations, e.g. the trap energy levels and wave functions, formation/transition energies etc. [8-14]. However, studies on the entire charge trapping process including the whole heterostructure and the related charge transfer dynamics all at ab initio level is much scarcer. One possible reason for such situation is that charge trapping phenomenon in MOSFETs has not been paid sufficient attention until Grasser et al. emphasized its importance to the bias temperature instability (BTI) in recent years [4,15-17]. Another reason is that such simulations on the whole heterostructures are often beyond the capability of the previous ab initio calculations methods and codes, and there are also other technical issues, ranging from interface structure, amorphous structure to how to calculate the charge transfer rates.

As discussed in one of our previous studies on charge trapping across Si/SiO_2 interfaces [18], the accurate atomistic simulation of the charge trapping process is possible only after a few technical challenges have been overcome. These include realistic interface structures, correct theoretical band alignment, and the application of adequate charge transfer theories. Undoubtedly, the existence of multiple interfaces will make the calculation even more challenging. First, the construction of atomistic models with multiple interfaces is difficult due to lattice mismatch of different materials. Second, the computational cost could be very high because a system with multiple interfaces is usually very large. Third, the increase of material types and interface numbers will greatly enhance the amount of possible defect candidates, including the defects in each material and the defects at each interface. A systematic study taking into account all the above factors will be a tall order. On the other hand, since the parameters needed to carry out a charge transfer calculation, e.g., the electron-electron coupling, the reorganization energy, and the

WKB decay length, are much less well known in multi-junction cases than the simple interface cases, this call for the development of a first principle calculation paradigm to solve this problem.

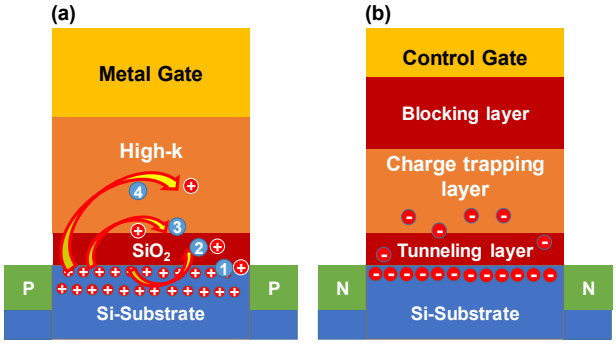

Fig. 1. Schematic of high-k MOSFETs (a) and charge trapping based nonvolatile memory cells (b). The multiple charge trapping paths are marked.

In this work, we combine the methods we have developed before into an optimized simulation framework, which is able to simulate the charge trapping process in most multiple interface systems, and then we apply it to the $Si/SiO_2/HfO_2$ gate stacks to investigate the hole trapping process along different paths in high-k gate transistors.

For charge trapping in HfO_2 dielectrics, it was demonstrated that oxygen vacancies (V_Os) should be the main charge traps because of their lower formation energies and closer energy levels with Si band edge [19,20]. While such conclusion is intuitively reasoned, it lacks a rigorous verification through quantitative calculations. The charge trapping from Si to HfO_2 in real high-k gate transistors is much more complicated. First, the high-k gate transistors always contain a thin SiO_2 interlayer between Si and HfO_2 so that the interface quality can be improved. Consequently, the energy level of oxygen vacancies in the $Si/SiO_2/HfO_2$ stacks will vary significantly depending on their locations, e.g. at the SiO_2 layer, at the SiO_2/HfO_2 interface, or at the HfO_2 layer, instead of being a constant [21]. Experiments have shown that there are different defect levels in HfO_2 gate stacks [22,23]. It has also been reported that double V_O could contribute more than single V_O to the random charging/discharging in HfO_2 [24]. Second, the energy barrier between defect level and the Si band edge is not the only factor that determines the charge trapping rate. The coupling strength between the two states also plays an important role [17,25]. It has been proved that the coupling strength is especially important when the initial state and final state are close in energy [18]. Third, the energy level of charge trapping defect in the dielectric layer depends greatly on the applied gate voltage, and so does the energy difference between these defect levels and the Si band edge. Finally, the Hydrogen(H) or Fluorine(F) passivation of the oxygen vacancy must be carefully considered because gas annealing is an indispensable process in transistor manufactory.

The framework proposed here will take all the important factors of charge trapping process into consideration, including atomistic interfaces, trapping energy barriers, coupling strength, electron-phonon interaction, oxide electric fields, and H/F passivation. With this framework, we manage to present the distinct hole trapping characteristics along different paths in the $Si/SiO_2/HfO_2$ stacks, and then reveal the mechanistic details of the charge trapping process, including which quantity controls the trapping rate most, what role the multiple interfaces and various passivation play, and where the dominant traps locate under different magnitudes of

electric field. Different with our previous work given in the conference [26], here we spend additional efforts on studying the Si/SiO_2 interface defects, and the effect of H and F passivation on all the V_O defects at Si/SiO_2 interface, SiO_2 bulk, SiO_2/HfO_2 interface, and HfO_2 bulk. We have also created an amorphous $Si/SiO_2/HfO_2$ interface stacks, which is more realistic compared with experiments and actual microelectronic devices to investigate the influence of structural disorder. These information are of great concern for industrial engineers, and have not been studied systematically. We have also provided much more details on Marcus theory and DFT calculations according to our systems. These theories and results will surely deepen our understanding on the charge trapping issue in high-k MOSFETs, and thus facilitate the solution of charge trapping problems in high-k MOSFETs and improve the integration of high-k materials in silicon CMOS technology.

II. THEORY AND SIMULATION

A. Marcus charge transfer theory

The charge trapping probability is determined by multiple factors, including the energy barrier between the initial and final state, the electronic coupling strength between the two states, and electron-phonon interactions. A well-recognized formula to describe such state-to-state charge transfer rate is the one proposed by R. A. Marcus in 1950's [27,28], which is able to take all the factors mentioned above into consideration:

$$\nu = \frac{2\pi}{\hbar}\left|V_C\right|^2 \sqrt{\frac{1}{4\pi\lambda k_B T}} \exp\left[-\frac{(\Delta G+\lambda)^2}{4\lambda k_B T}\right] \qquad (1)$$

where V_C is the coupling constant between initial state and final states, ΔG is the total Gibbs free energy change for the charge transfer reaction, and λ is the reorganization energy that stems from the structural relaxation caused by charge trapping. It represents the strength of electron-phonon coupling. This Marcus formula has been successfully applied to semiconductor-molecule systems to study the electron and hole transfer dynamics [25,29,30].

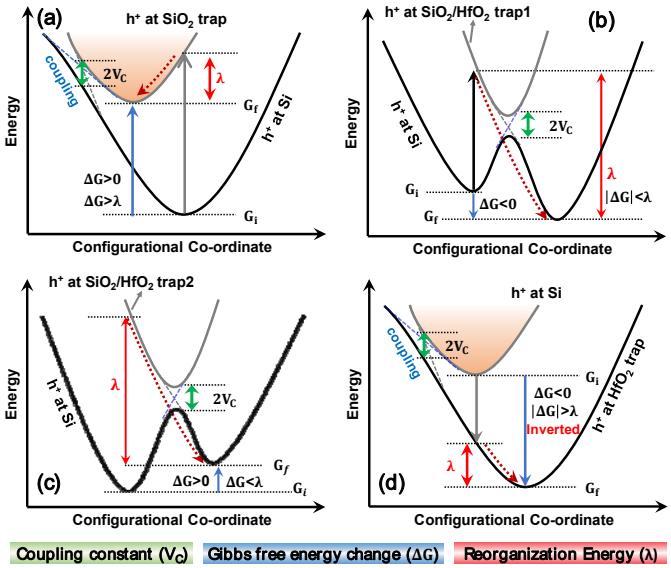

Fig. 2. The energy diagrams in configuration space for hole trapping from Si to the oxygen vacancy trap in (a) SiO_2, (b) SiO_2/HfO_2 interface trap1, (c) SiO_2/HfO_2 interface trap2, and (d) HfO_2. The three key factors in Marcus theory are marked in each case. The two SiO_2/HfO_2 interface defects are marked and distinguished in Fig. 3.

The schematic description of Marcus theory and the charge trapping process is shown in Fig.2, in which the horizontal axis represents structural configuration, and the vertical axis is the energy of different configurations. According to the relative magnitude of G_f and G_i, and the relative magnitude of ΔG and λ, the energy diagram of Marcus charge transfer theory can be divided into different situations. The four schematics shown in Fig. 2 represents the charge trapping process from Si to SiO_2, SiO_2/HfO_2 interface and HfO_2 respectively, and all of them are results by the DFT calculations conducted in this work, which will be shown later. For the following conceptual discussion, any one of the four schematics can be used as the reference. At the beginning of the hole trapping process, a hole lies on the valence band maxima of Si (VBM_{Si}), and the energy of the system can be written as

$$G_i = E_0 - VBM_{Si} - \lambda_{Si} \quad (2)$$

where E_0 is total energy of the charge neutral system, and λ_{Si} is the reorganization energy caused by structural relaxation when VBM_{Si} is occupied by the hole. Then the hole transfers to the defect by crossing the energy barrier between VBM_{Si} and the defect level (E_{defect}). Such a transition is induced by the coupling constant (V_C) between VBM_{Si} and E_{defect}. After the hopping, the atomic positions will experience a structural relaxation due to the occupation of the defect level by a hole, and the final energy of the system becomes

$$G_f = E_0 - E_{defect} - \lambda_{defect} \quad (3)$$

where λ_{defect} is the reorganization energy caused by the structural relaxation of atoms around the defect.

Since the wave function of VBM_{Si} is very delocalized, the structural relaxation caused by hole occupation in VBM_{Si} should be negligible, and thus λ_{Si} is treated as zero. On the contrary, the λ_{defect} is usually large due to the localized nature of defect states and the strong electron-phonon coupling. Therefore, the Gibbs energy change of the hole trapping process can be written as:

$$\Delta G = G_f - G_i = VBM_{Si} - E_{defect} - \lambda_{defect} \quad (4)$$

The overall λ can also be taken as λ_{defect} if we ignore $\lambda_{Si.}$ With the meanings of ΔG, λ, and V_C known, the difficulty lies on how to calculate them accurately in a Si/SiO_2/high-k system. First, we should build a structure with explicit interface so that the effect of such multiple interfaces can be studied thoroughly. Second, we must conduct high-accuracy DFT calculation on the whole interface system to obtain the correct band gap and band alignment. This is very important for charge trapping simulation because the charge trapping rate depends exponentially on the energy barrier between silicon band and defect levels. For this purpose, we like to use the Heyd-Scuseria-Ernzerhof (HSE) hybrid exchange-correlation functional instead of LDA or GGA, because the latter ones usually underestimate the band gap [31]. Third, a more direct method should be used to obtain the coupling constant accurately, under the realistic atomistic environment, especially with atomistic interfaces taken into considerations. Finally, a hole should be precisely inserted (trapped) to the targeted defect level as to obtain the correct reorganization energy. With all these key quantities obtained, the state-to-state hole trapping rate can be calculated using Eq. (1).

B. Atomistic models

We first construct two $Si/SiO_2/HfO_2$ interface models that are shown in Fig. 3(a) and (b), which differs with each other at the thickness of the SiO_2 interlayer. The phase of the SiO_2 and HfO_2 is β-cristobalite and monoclinic, respectively, and the orientation of the structure is (001). The side length of the unit cell is set as 10.86×10.86 $Å^2$, which is the size of the relaxed Si part. The strain of the SiO_2 part with respect to the Si and HfO_2 part is -6.69% and -2%, respectively. These settings are chosen and determined by carefully referencing previous works [21,32-34]. The effect of strain on defect formation energy can be found in several recent works [35, 36]. The marked oxygen atoms in Fig.3 are the oxygen vacancies that have been studied in this work. Each defect is denoted by a phrase combining defect location with the defect order number. For example, Si/SiO_2-1 is the first defect at the Si/SiO_2 interface. To reveal the important role of dangling bonds at the Si/SiO_2 interface, and in seeking for a solution to weaken the trapping capability of the dominant hole traps, we have also attempted to passivate all the oxygen vacancies by H and F atoms. Lastly, we create an amorphous $Si/SiO_2/HfO_2$ structure ($cSi/aSiO_2/aHfO_2$) by MD simulations through the melt-quench process, to study the statistical property of charge trapping in disordered system. Six interfacial oxygen vacancies and eight HfO_2 oxygen vacancies are sampled and labeled in Fig. 3(c). We note that a metal gate could affect the work function at the metal/HfO2 interface [37], but it will not change the physical picture of charge trapping from Si to the trap states in SiO_2 and HfO_2 layers.

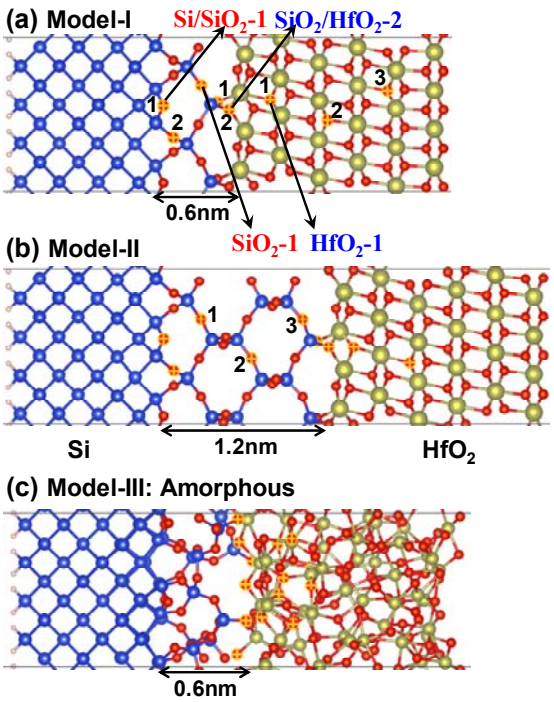

Fig. 3. (a) and (b) Two (001) oriented $Si/SiO_2/HfO_2$ gate stack models with 0.6 and 1.2 nm interlayer, respectively. Oxygen vacancies at different locations, i.e. Si/SiO_2 interface, SiO_2 interlayer, SiO_2/HfO_2 interface, and HfO_2 high-k layer, are numbered separately. (c) The $cSi/aSiO_2/aHfO_2$ stack used for statistical study.

The MD simulation is carried out by the QuantumATK 2018.6 [38,39] (ATK), and the force field is from Ref [40]. Langevin thermostat is adopted in the whole melt-quench process, and a timestep of 1 fs is used. The melt process begins with an enlarged supercell, as references usually do [41,42], to facilitate the bond breaking, and it lasts for 50 ns under the temperature of 5000 K. After that, the supercell is shrunk back and melt for another 50 ns under 5000K. Finally, the system is cooled down linearly from 5000 K to 300 K within 500 ns, i.e. a cooling rate of 9.4 K/s, to get the final structure. One tricking thing is that the SiO_2 and HfO_2 will mix with each other if we start the melting with the whole crystalline interface structure. To avoid that, we need to begin with a crystalline Si/SiO_2 stack and get the crystalline-Si/amorphous-SiO_2 first, and then put the crystalline HfO_2 into the supercell and melt the HfO_2 while keeping the SiO_2 part fixed.

The quality of the amorphous HfO_2 is confirmed by checking the coordination of each atom and the radial distribution function (RDF) of them, which are shown in Fig. 4. In agreement with previous theoretical and experimental works [43-45], the coordination number of Hf atom is dominated by 6 while accompanied by a few 5 and 7, and that of the O atom is dominated by 3 with a few 2 and 4. The 1-coordinated O atom is the ones at the SiO_2/HfO_2 interface, who bridge the Si and Hf atoms. Also in consistent with previous works [46-48], the Hf-O RDF peaks at about 2.1 Å, while that of O-O and Hf-Hf distribute around 2.8 Å and 3.5 Å.

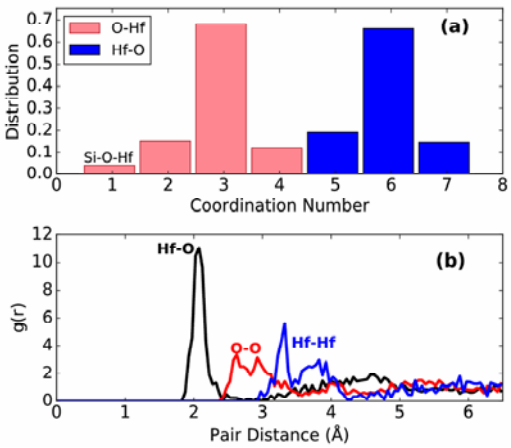

Fig. 4. The coordination number and the radial distribution function of the amorphous HfO_2 part.

C. Density-functional theory simulation

DFT simulations are carried out by the plane-wave package PWmat with GPU acceleration [49,50]. GGA-PBE functional is used for structural relaxation with a convergence criterion of 0.01 eV/Å for the residual force. Hybrid HSE functional is used in all the self-consistent field (SCF) calculations to obtain the correct band alignment and defect levels. HSE functional is also used in calculating the reorganization energy to correct the PBE results. The SG15 norm-conserving pseudopotentials are adopted with an energy cutoff of 50 Ry. Single Gamma point is sampled considering the large superlattices and large number of atoms in each model. HSE parameters are set separately with a mask function for different materials to obtain their correct band gaps simultaneously [51]. The parameter sets for bulk Si, SiO_2, and HfO_2 are determined by reproducing their reported band gap of 1.12 eV, 8.5 eV, and 5.8 eV, respectively. With these parameters, the band alignment of the $Si/SiO_2/HfO_2$ interface structure are obtained and shown in Fig. 5. It can be seen that the band gaps that agree well with experiment values are realized simultaneously. Besides, it is found that the interface transition regions are not atomically sharp. Therefore, the local atomic nature of interfaces must be considered in a realistic simulation of the multi-interface gate stacks.

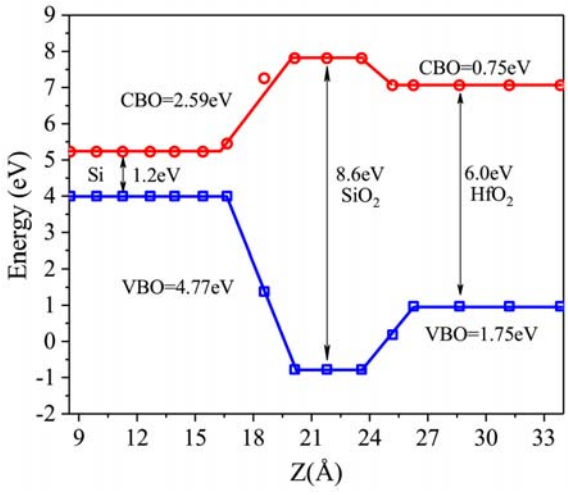

Fig. 5. The band alignment of $Si/SiO_2/HfO_2$ system (model-II) calculated by density-functional theory with hybrid functional (HSE). CBO/VBO: conduction/valence band offset.

The reorganization energy λ for each defect is obtained by inserting a hole into the defective system, and then relax the system and record the energy change. Since this relaxation is a local effect, we can calculate it based on a pure bulk SiO_2 and HfO_2, or with the SO_2/HfO_2 interface system without Si. This has the advantage that the defect level will be inside the band gap, thus will not hybridize with the Si inside-band states, which can make the charged defect atomic relaxation intractable. More specifically, we first relax the atomic structure with defect at its neutral state (N electrons) and obtain an atomic structure R_0. Then, we remove an electron from the R_0 structure (N-1 electrons), and without relaxation the atomic positions, carry out an electronic structure self-consistent calculation to obtain the total energy $E(R_0, N\text{-}1)$. The electron is in fact removed from the defect level, because the defect level lies at the band gap and is the highest occupied level. After that, we relax the atomic structure with N-1 electrons to obtain its minimum energy $E(R_1, N\text{-}1)$. The energy differences between these two atomic configurations (both with N-1 electrons) is the reorganization energy:

$$\lambda = E(R_0, N\text{-}1) - E(R_1, N\text{-}1) \tag{5}$$

Note, since both energies have N-1 electron, they both have electrostatic image energies, thus there is no need for image interaction correction. The uncertainty caused by this electrostatic image interaction for the calculation of λ should thus be much smaller than the typical defect level calculations where $E(N+1)$ and $E(N)$ are subtracted.

The Gibbs free energy change ΔG can be obtained straightforwardly according to Eq. (4) once the band alignment, defect levels and reorganization energy are known. The most difficult but important task is to calculate the coupling constant V_C. In previous literatures, the V_C is often obtained by using the WKB approximation [16,17]:

$$V_C = k_t \exp(-\frac{\sqrt{2m_t \Delta E}}{\hbar} d) \tag{6}$$

where ΔE is a tunneling barrier, m_t is the tunneling effective mass and the parameter k_t can only be obtained by calibration with experiments. Such approximation treats the coupling of two states as the tunneling of one state to the other, and it is not capable of taking into account the explicit atomic environment. Moreover, the WKB approximation has only been used in single-interface systems such as Si/SiO_2, and its validity in multiple-interface systems is quite questionable (as the wave function can be bounced by at the interface). Even in single-interface Si/SiO_2 system, our previous work has shown that the WKB approximation can underestimate the coupling strength of two states [18].

In our more accurate approach, V_C will be obtained by direct DFT calculations. Considering a two-state system with coupling constant V_C that is subjected to an external field, we can write down the Hamiltonian of the system by denoting the original energy difference of the two levels as $\Delta\varepsilon_0$, and the field induced potential change as F:

$$H = \begin{pmatrix} -\Delta\varepsilon_0 / 2 + eF & V_C \\ V_C & \Delta\varepsilon_0 / 2 - eF \end{pmatrix} \quad (7)$$

Diagonalizing this 2x2 Hamiltonian, we can obtain the eigen energies of these two states as:

$$\varepsilon_{\pm} = \pm\sqrt{V_C^2 + (\frac{\Delta\varepsilon_0}{2} - eF)^2} \quad (8)$$

It can be seen that the two levels will get closer to each other under certain field, but they will never cross each other due to their coupling. The minimum energy gap of the two levels is found to be exactly two times of the coupling constant V_C. Guided by this theory, we intentionally apply an electric field to the $Si/SiO_2/HfO_2$ structure, and to drive the VBM_{Si} and E_{defect} close to each other until the anti-crossing (avoid crossing) phenomenon occurs.

In summary, the theoretical simulation framework contains two steps. First, carrying out DFT calculations to obtain the parameters needed by Marcus theory, and then input them into the Marcus charge transfer formula to get the exact trapping rate. The work flow of this scheme is shown in Fig. 6. With this framework, we can now investigate the charge trapping process in any multilayered structures.

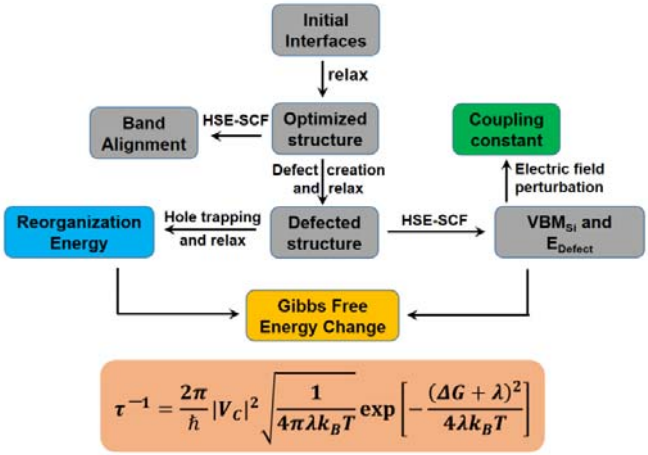

Fig. 6. The flowchart of the theoretical simulation framework, including the sophisticated DFT calculations, and the Marcus charge trapping theory.

III. RESULTS AND DISCUSSION

From Eq. (1), it can be seen that the hole trapping from VBM_{Si} to a defect in the dielectric layer is more likely to happen when the defect level is close to the VBM_{Si}, and when the coupling constant between the two states is large. However, as we will show below these two conditions are usually against each other, hence it is difficult to be satisfied at the same time. The balance between these two factors dominates the story of hole charge trapping in the $Si/SiO_2/HfO_2$ system.

A. Defect level and Si band edge alignment

Fig. 7 summarizes the defect level alignment of multiple-source V_O centers with respect to

the Si band edge. Obviously, the V_O defects at different positions produce distinct defect levels. First, we find that the V_O defects at the Si/SiO_2 interface will not induce any local defect states near the VBM_{Si} unless a hydrogen atom is introduced. Second, the V_O defects inside the SiO_2 interlayer are deeply below the VBM_{Si}, indicating that they are rarely able to trap holes. Third, those at the SiO_2/HfO_2 interface also lie below VBM_{Si} but are much closer to VBM_{Si} in energy, which means that they are more advantageous in hole trapping. Last, the V_O defects at the HfO_2 layer lie very slightly above VBM_{Si}, making them the most energetically favorable hole traps. Nevertheless, it is worth mentioning that all the defect levels will be raised up by negative bias temperature instability (NBTI) stresses for a *p*-type FET where the hole trapping takes place. So the hole trapping capability will change according to the gate electric field amplitude.

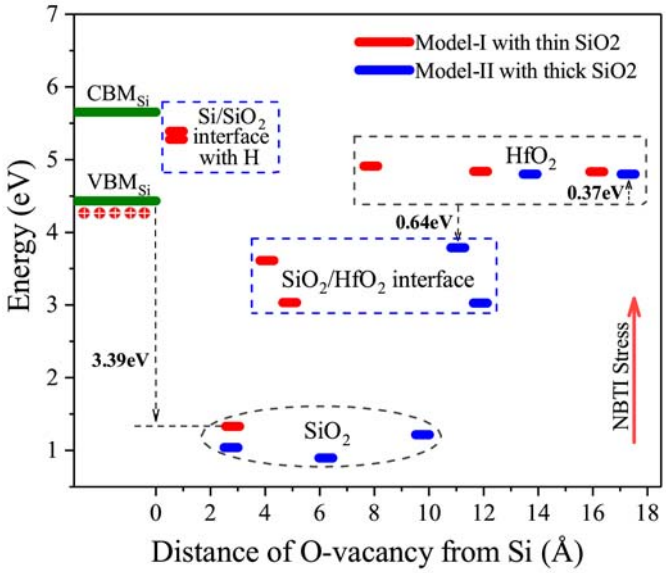

Fig. 7. The defect level alignments of multiple-source V_O centers with respect to the Si band edge. The V_O defect state at the Si/SiO_2 interface is not local unless an H atom is induced.

B. VBM_{Si}-E_{defect} coupling

Fig. 8 depicts the coupling and anti-crossing energy curves between VBM_{Si} and two V_O defects. The two V_O defects vary in location and their distance from Si, and thus couple with different strength with VBM_{Si}. For the first defect at the SiO_2 interlayer, as is shown in Fig. 8(a), it can be seen that the wave function of the E_{defect} is significantly localized at the oxygen vacancy before a strong coupling, and VBM_{Si} is much more delocalized at the Si atoms. With further approaching of the two energy levels, their wave functions begin to overlap with each other, and they localize at the same position when they couple the most. After that, these two states separate apart, and the characters of VBM_{Si} and E_{defect} state will be switched. From the minimum gap of these two curves, one can obtain the 2Vc amplitude. The second defect shown in Fig. 8(b) is a defect at the HfO_2 layer. The coupling process is nearly the same as that in Fig. 8(a), but the coupling constant is much smaller in value. This is because the V_O defect at HfO_2 is farther away from silicon, and there is an interface in between.

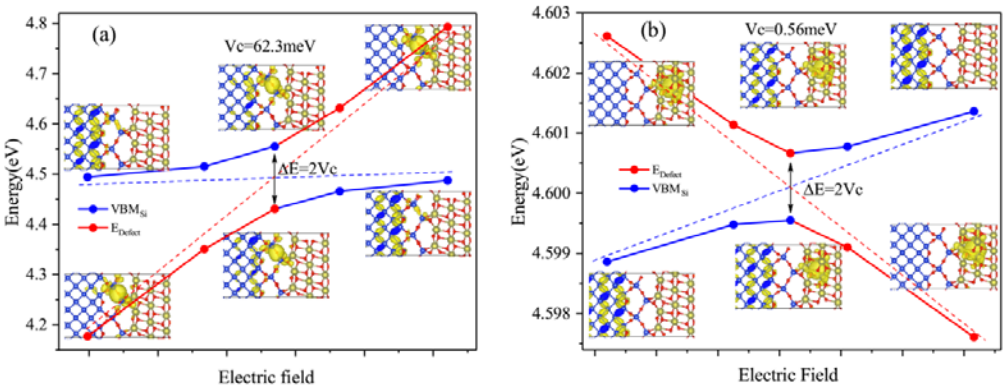

Fig. 8. The coupling process of VBM_{Si} with V_O defect in (a) SiO_2 interlayer, and (b) HfO_2 high-k layer

The coupling constants of VBM_{Si} with all the other V_O defect levels are obtained by the same procedure and are shown in Fig. 9. Obviously, the coupling constants decrease monotonically with the distance of the defects from the Si substrate. However, it is also evident that the decay behavior of V_C can be divided into three types according to the V_O defect locations. First, it can be seen from Fig. 9(b) that the V_C decay at the SiO_2 interlayer follows a good exponential trend with a decay length of 1.58 Å. However, it will experience a sharp drop when encountering the SiO_2/HfO_2 interface. If we put the interface defects of the two models together, as is seen in Fig. 9(c), we can also see an exponential trend but with a different scaling length (1.92 Å). More importantly, we find from Fig. 9(a) that the V_C decay in the high-k HfO_2 layer doesn't follow a simple exponential law. These results mean that the coupling constant decay in a single interface system, e.g. Si/SiO_2, can be qualitatively described by a simple exponential function such as WKB approximation, but the V_C decay in multi-interface high-k stacks, e.g. $Si/SiO_2/HfO_2$, is more complicated, and it can't be described by a simple exponential function.

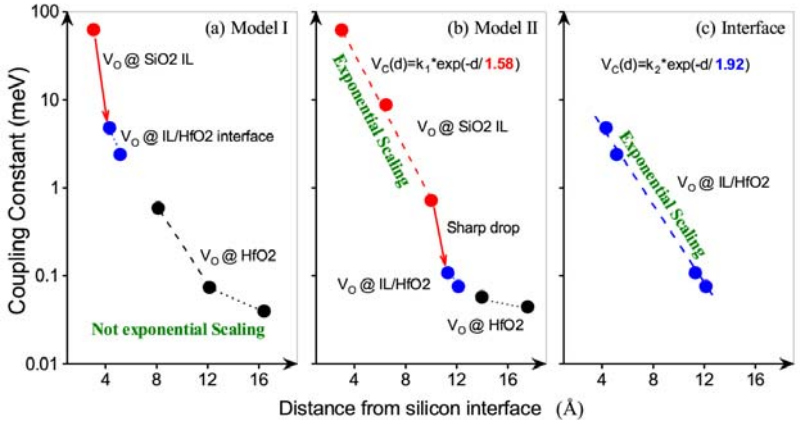

Fig. 9. The decay of coupling constant with the distance of V_O defect from Si substrate.

C. Reorganization energy

The effect of electron-phonon interaction is included in the reorganization energy, i.e. the energy change caused by structural relaxation after charge trapping. Fig. 10 illustrates the

reorganization process for three typical V_O defect locations. There is a common feature that all the atoms around the vacancy defect will depart more from each other after hole trapping. However, the reorganization energy value differs because of the different local environment. By using PBE functional, it is found that the V_O defect at the SiO_2 interlayer has the reorganization energy of 0.31 eV, while the SiO_2/HfO_2 interface, and HfO_2 V_O defects have values around 1 eV.

Although these DFT results are expected to be relatively correct, it is always puzzling us that whether the choice of functional (e.g. PBE and HSE) will affect the calculation of the reorganization energy, especially because the level of charge localization and polaronic energy depend on the functional used, and sometimes PBE gives delocalized solutions when the physically correct picture is that of a localized charge.

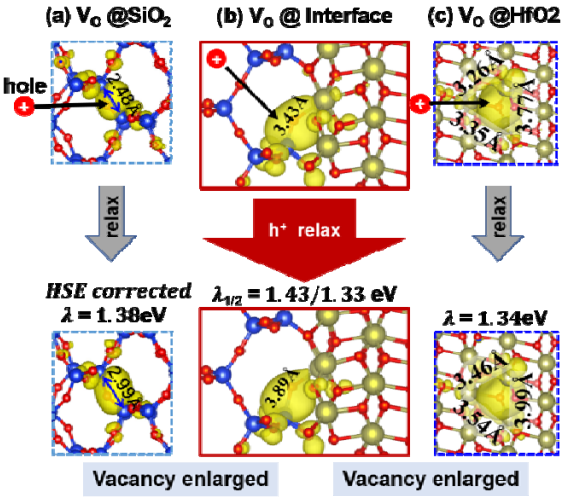

Fig. 10. The structural relaxation after hole trapping and the reorganization energy for V_O defects at (a) SiO_2, (b) SiO_2/HfO_2 interface, and (c) HfO_2. All the values are corrected by HSE functional calculations.

To answer this question, we build two smaller models containing 96 atoms, of which one is crystalline HfO_2 and the other one is SiO_2, so that the structural relaxation by HSE functional is available. Then we sampled two V_O defects (3-coordinated and 4-coordinated) in HfO_2 and one V_O defect in SiO_2 to calculate the reorganization energy with PBE and HSE functional, respectively. See Fig. S1-S3 in the Supplemental Material for the models and detailed comparison results [52]. It is found that the HSE functional generally produces larger reorganization energy than the PBE functional. For both kinds of V_O defects in HfO_2, the HSE result is larger than the PBE result by a factor of about 1.4. For the V_O defect in SiO_2, when we calculated the electronic structure using PBE functional under the neutral defect atomic positions, but occupying it with one hole (thus making it a "+" charged state), due to state hybridization with VBM state, after SCF steps, the hole is not staying in the localized defect state as the one shown in Fig.10(a), instead it occupies a delocalized state, which changes the physical meaning for reorganization energy. To correct this problem, we have forced the hole in the original localized defect state (from the neutral state SCF calculation) in a constraint DFT scheme, and keep the hole state unchanged during SCF iterations. The atomic relaxed "+" charged state does not have this problem, thus can

be calculated in more conventional way. The so calculated PBE reorganization energy is 0.99 eV, which is also about 1.4 times smaller than the corresponding HSE result (1.38 eV). We have also tested the effect of functional on the H-passivated V_O defects, and found a slightly different ratio between PBE and HSE results. See Fig. S4-S5 in the Supplemental Material for the simulation results [52].

In summary, the PBE function always produces smaller reorganization energy than the HSE functional probably due to larger wave function delocalization, but the PBE results can be approximately corrected by multiplying an amplification factor that depends on the defect type. For Vo defect in SiO_2 and HfO_2, the correction factor is 1.4, while for Single-H passivated defect, the correction factor is 1.1, and for Double-H passivated defect, the correction factor is 1.3.

D. Hole trapping rates

With all the decisive parameters obtained, the hole trapping rates can be calculated by using Eq. (1). The trapping rates to the V_O defects at SiO_2 interlayer are too small to be shown here, so there are only data for V_O defects at SiO_2/HfO_2 interface and the HfO_2 layer in Fig. 11. First, we can discuss the case when gate voltage is zero. It can be seen that the trapping rates to the HfO_2 layer V_O defects are very high, but not always the highest, even though these V_O defects are closest to VBM_{Si} in energy. This is because they are very far away from the Si substrate, thus their coupling with VBM_{Si} is very weak. On the contrary, the V_O defects at the SiO_2/HfO_2 interface couple much stronger with VBM_{Si} due to smaller distance with Si, so their hole trapping capability can be stronger even though their energy barrier with VBM_{Si} is less favorable for hole trapping. These results manifest well in the balance between coupling constant and energy barrier in controlling the charge trapping rate. Overall, the energy barrier between VBM_{Si} and E_{defect} is more dominant because it appears at the exponential component in Eq. (1).

In a MOSFET, the hole trapping is always electric field-dependent. The oxide electric field will change the alignment of the defect level with respect to the VBM_{Si}, and thus also change the energy barrier

$$\Delta G = VBM_{Si} - (E_{defect} + F_{OX} \cdot d) - \lambda_{defect} \quad (9)$$

where F_{OX} is the electric field induced by negative gate voltage, and d is the distance between Si substrate and the V_O defect. Taking this re-alignment into account, the F_{OX}-dependent hole trapping rates are calculated and also shown in Fig. 11. Since all the defect levels will be raised up by the NBTI stresses, the interfacial V_O defects will get closer to VBM_{Si} and become more energetically favorable for hole trapping. As a result, their trapping capability will become stronger. On the contrary, because the V_O defects at the HfO_2 are already higher in energy than VBM_{Si} at zero electric field, the NBTI stress will further drag the energy level away from VBM_{Si}, which eventually enters the Marcus inverted region so their trapping capability will be decreased [53]. Nevertheless, the V_O defects in HfO_2 layer will always stay effective because the electric field in high-k layer is usually very weak.

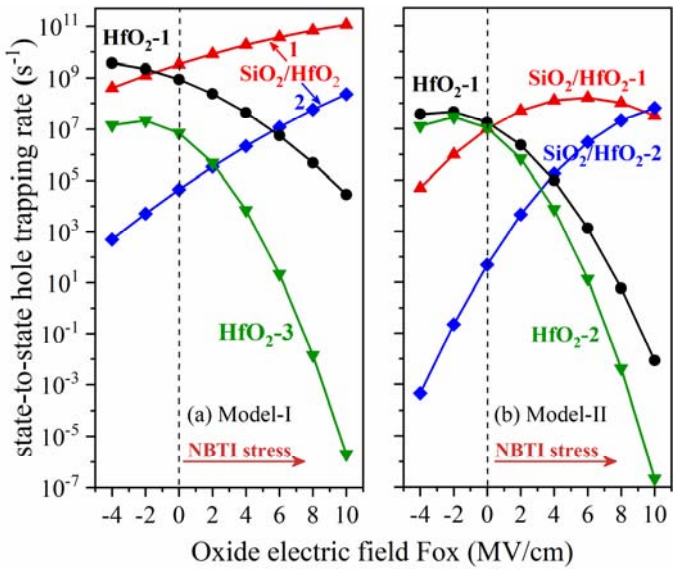

Fig. 11. The F_{OX} dependent hole trapping rate for different V_O defects in the case of model-I and model-II.

E. Complicated effect of H and F passivation

The effect of Hydrogen (H) and Fluorine (F) passivation on defect charge trapping is very complex and interesting. On the one hand, it is widely known that proper passivation is able to reduce defect state density so to relieve the charge trapping phenomenon [54-56]. On the other hand, it is also found that the forming and breaking of Si-H bond at the Si/SiO_2 interface play an important role in charge transfer and BTI [57,58]. Moreover, the F passivation is reported to be different from H passivation in relieving charge trapping in high-k MOSFETs [59-61]. These phenomena naturally give rise to many questions such as why H passivation is not as good as F in relieving charge trapping? Why H atoms are important for charge trapping at the Si/SiO_2 interface? In addition, is the effect of passivation the same for defects that locate at different part of multilayer high-k gate stacks? We will like to use our theoretical simulations to help to answer these questions.

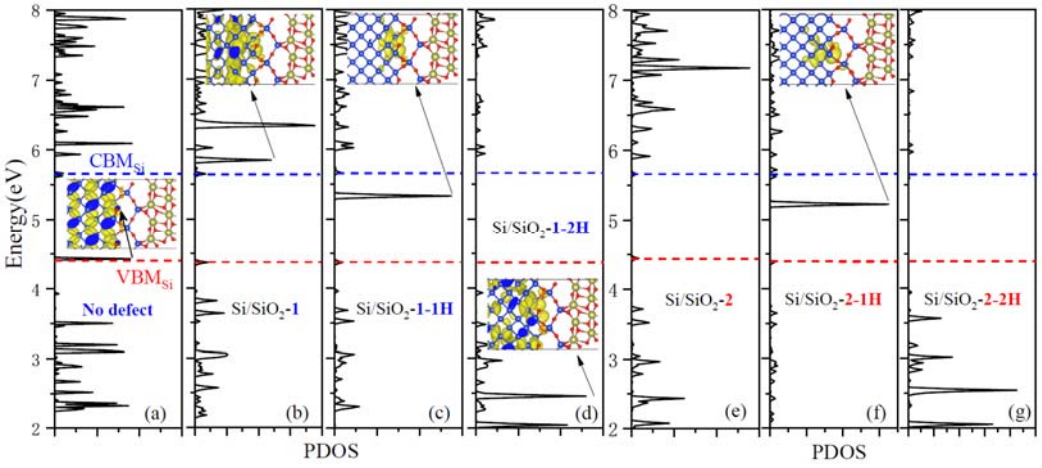

Fig. 12. PDOS and wave function of oxygen vacancies at the Si/SiO_2 interface. (a) No vacancy, (b) 1^{st}-Vo type with no passivation, (c) 1^{st}-Vo type with single H passivation, (d) 1^{st}-Vo type with double H passivation, and (e)-(g) 2^{nd}-Vo type.

First, we take a look at the effect of H atoms on the V_O defects at the Si/SiO_2 interface. It can be seen from the models in Fig. 3 that there are two kinds of V_O defect at the Si/SiO_2 interface according to their local bonding environment. The first Si/SiO_2 V_O defect lies between two Si atoms that belong to the bulk silicon, and the second V_O defect lies between bulk Si and SiO_2. The energy levels of these two defects before and after H passivation are all obtained by checking the partial density of states (PDOS) of the atoms around the defect, and are shown in Fig. 12. As mentioned in part III-A, there are no strongly local defect states inside or near the band gap when the defect is not passivated, as is seen in Fig. 12(b). Two strong PDOS peaks slightly above the Si CBM might indicate defect states. However, a closer investigation of the actual states near those energy shows that not only they have strong charge at the defect site, but they also have charge density in the Si. It is possible the defect state is hybridized strongly with bulk Si state. The case of V_O defects with double H passivation is also similar, as shown in Fig. 12(d). For the double H passivation, the PDOS peaks are far below the VBM, indicating the passivation has pushed them all the way from conduction band into valence band. In contrast, for the Vo with only one H, the defect state has been pushed down, from above CBM into the band gap, but not all the way into the VB, as shown in the PDOS of Fig.12(c). As a result, the corresponding wave function is very localized. Such phenomenon has also been observed in the second Si/SiO_2 interface defect, as is shown in Fig. 12(e)-(g). All these show a complicated story of H passivation at the Si/SiO_2 interface.

Following the framework shown in Fig. 6, the hole trapping rates from VBM_{Si} to these Single-H passivated Si/SiO_2 interface defects are obtained and shown in Fig. 13(a). In comparison with the main hole trapping centers shown in Fig. 11, we find that these Si/SiO_2 interface defects are weaker in hole trapping under NBTI stresses. The reason is multifold. First, the energy barrier of H passivated Si/SiO_2 interface defects is much larger than those at the HfO_2 layer, as can be seen in Fig. 7. Second and more importantly, the reorganization energy of H passivated Si/SiO_2 interface defects are found to be very small, as is shown in Fig. 13(b) and (c). They are only 1/3 to 1/2 of those unpassivated Vo at SiO_2/HfO_2 interface and HfO_2 layer. Moreover, their trapping capability is further weakened by the NBTI stresses because the defect levels lie above VBM_{Si}, which will be raised up, further increase the energy barrier.

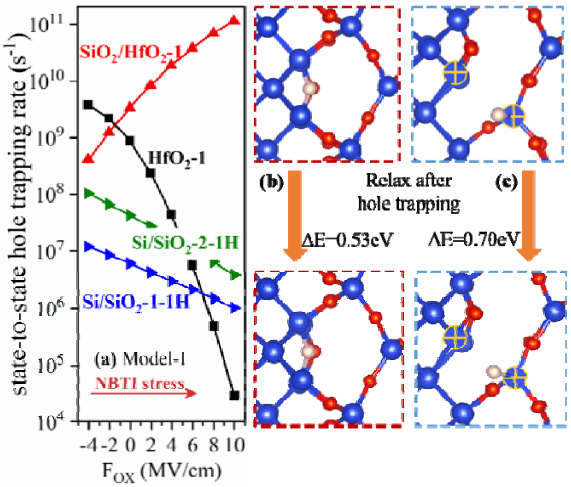

Fig. 13. (a) Comparison of hole trapping rate from VBM_{Si} to V_O defects at SiO_2/HfO_2 interface, HfO_2, and H-passivated Si/SiO_2 interface; (b) and (c) The reorganization of the two kinds of V_O defects at the Si/SiO_2 interface, both with single H passivation.

In contrast to the Si/SiO_2 interfacial V_O defects, the V_O defects in other locations will directly induce a very localized defect state near the VBM_{Si}, as has been shown in Fig. 7 and Fig. 10. Therefore, the effect of passivation on these locations is supposed to be very different from that on Si/SiO_2 interface. Along with the purpose to distinguish the effect of H and F passivation, we carry out study on H and F passivation on V_O defects in all locations.

Fig. 14(a) shows the energy alignment of Si band edge and the H passivated V_O defects at different locations. Both Single-H passivation and Double-H passivation are studied. Compared with the defect levels without passivation (denoted by gray star-lines), it can be seen that Single-H passivation will push all the V_O defect levels upwards while Double-H passivation will pull them down. Besides, the localized defect state will disappear when the V_O defects at SiO_2 are passivated by double H atoms. Nevertheless, neither Single-H passivation nor Double-H passivation is able to completely eliminate the hole trapping problem. For Single-H passivation, the SiO_2 V_O defect and the 2nd SiO_2/HfO_2 interface V_O defect are close to VBM_{Si}, and thus are effective traps. The Double-H passivation is better in relieving hole trapping, but the 1st SiO_2/HfO_2 interface V_O defect and the HfO_2 V_O defect are still not far from VBM_{Si}, and thus are likely to be effective traps. We next calculated the coupling constants and reorganization energy of each defect, which are shown in Fig. 14(b). The resulting hole trapping rate under different magnitude of electric field are shown in Fig.14(c). Under negative gate voltages, it can be seen from Fig. 14(c) that the Vo-1H at the SiO_2 layer and the Vo-2H at the SiO_2/HfO_2 interface will both be active hole trapping centers.

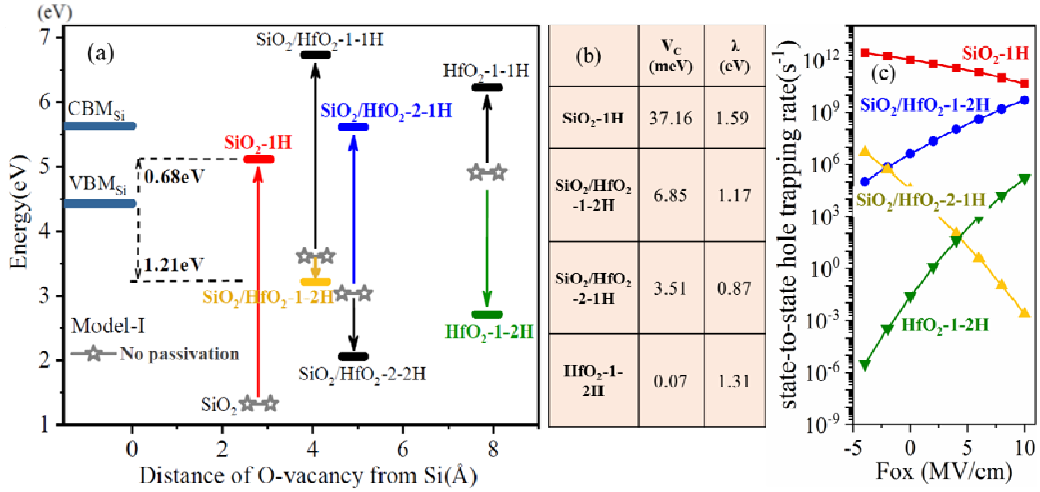

(b)	V_c (meV)	λ (eV)
SiO_2-1H	37.16	1.59
SiO_2/HfO_2-1-2H	6.85	1.17
SiO_2/HfO_2-2-1H	3.51	0.87
HfO_2-1-2H	0.07	1.31

Fig. 14. (a) the energy alignment of V_O defects and the Si band edge before and after passivation, (b) the coupling constant and reorganization energy of each V_O defect, (c) the electric field dependent hole trapping rate from VBM_{Si} to four V_O defects that most likely to be traps.

The effect of F passivation is found to be very different from H passivation. It can be seen from Fig. 15(a)(b)(c) that a single F atom can perfectly replace the O atom regardless of the location at the SiO_2 layer, the SiO_2/HfO_2 interface, or the HfO_2 layer. This is a bit surprising since one might think a single F^- anion cannot replace an O^{2-} anion. Since there is no dangling bond with F passivation, there is also no obvious defect energy near the Si band edge, as is seen in Fig. 15(d). The defect levels induced by a Single-F passivation is far from the Si band edge, and thus will not be able to trap holes according to Eq. (1). The Double-F passivation present several different features. First, the relaxed locations of F atoms are different with Single-F passivation. Second, the two F atoms will induce two localized states that close in energy, as can be seen in Fig. 15(e). The two states differ at the charge density distribution. Despite these differences, we can clearly see the common feature that no localized state that close to Si band edge will be induced by F passivation. Consequently, the hole trapping problem can be greatly relieved by F passivation, which is in consistent with experimental observation [60].

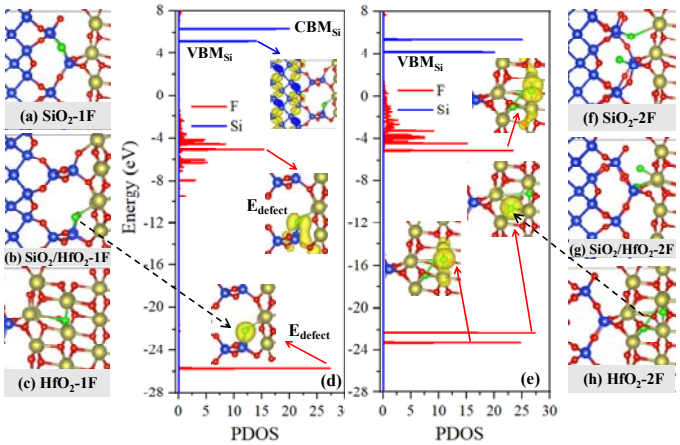

Fig. 15. The relaxed structures of F passivated V_O defects and their PDOS. (a)(b)(c) Single-F

passivation in SiO_2, SiO_2/HfO_2 interface, and HfO_2, respectively. (f)(g)(h) Double-F passivation in each position. (d) The PDOS of the Single-F atom at SiO_2/HfO_2 interface. (e) The PDOS of the two F atoms at HfO_2.

F. Charge trapping variation in amorphous $Si/SiO_2/HfO_2$ stack

Although we have pointed out the distinct charge trapping characteristics of defects at SiO_2, HfO_2, and their interfaces, respectively, one could still concern what happens in more complicated but more realistic amorphous $Si/SiO_2/HfO_2$ stacks. The local environment in amorphous ones could be very different even for the same kind of defects in the same material, not to mention the interfaces. We note that the defect level of oxygen vacancy in an amorphous $Si/SiO_2/HfO_2$ stack was reported before [62], but no further study on charge trapping or statistical study on the defect level variation was carried out. Therefore, we create the amorphous $Si/SiO_2/HfO_2$ stack shown in Fig. 3(c) to reveal the charge trapping variation in disordered system, and to look for the information that can not be extracted from crystalline ones. As marked in Fig. 3(c), we sampled six interface V_Os defects and eight HfO_2 bulk V_Os. We have also created a puckered V_O defect in SiO_2, as is shown in the inset of Fig. 16, which has been proved to be exist in amorphous silica [63,64]. Then we calculate their defect levels, coupling constant with VBM_{Si}, reorganization energy, and finally the hole trapping rates under different magnitude of electric fields.

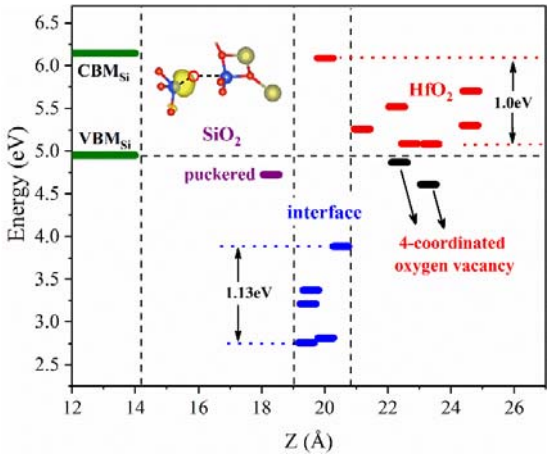

Fig. 16 The defect levels of the oxygen vacancies in $cSi/aSiO_2/aHfO_2$.

The defect level of each V_O sample is shown in Fig. 16. Compared with the results in crystalline stacks, the consistent phenomenon is obvious, i.e. the defect levels induced by SiO_2 V_O defects and SiO_2/HfO_2 interface V_O defects are all below the VBM_{Si}, and those induced by HfO_2 V_O defects are mostly above the VBM_{Si}. On the other hand, several new phenomena are also easily noticed. First, the puckered V_O defect in SiO_2 is much closer to VBM_{Si} compared with the common dimer ones in crystalline SiO_2. Second, there are several 4-coordinated V_O defects in the $aHfO_2$ whose defect level is slightly below the VBM_{Si} instead of inside the Si band gap. Third, the defect levels at each material exhibit strong variation, which is accessible considering the disordered local environment in amorphous structures.

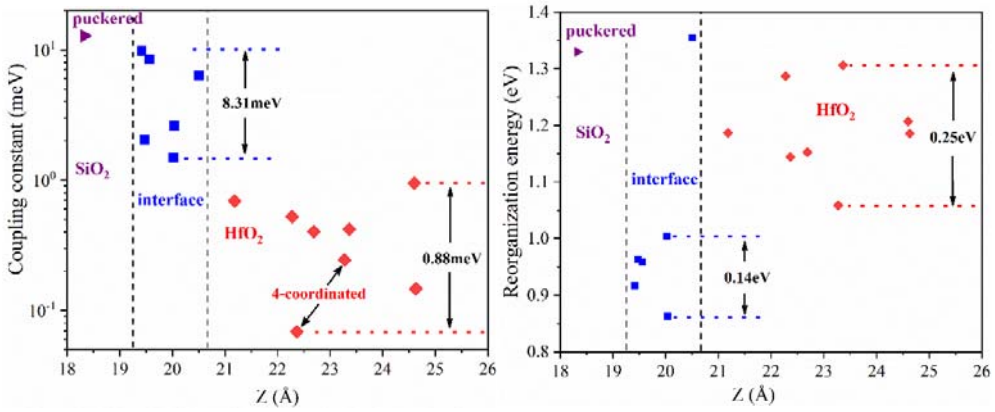

Fig. 17 (a)The coupling constant of each defect level with VBM_{Si}, (b) the reorganization of each defect after hole trapping. All the reorganization data are corrected by HSE functional calculation.

The variation also shows itself in the coupling constants and reorganization energy of each defect in Fig. 17. For the coupling constants shown in Fig. 17(a), we can still see a decrease trend with the increasing distance of defect from Si, which is consistent with the case in the crystalline stack, but the trend is not strictly followed by every point. For the reorganization energy, the fluctuation is also obvious even though the magnitude is less than one order.

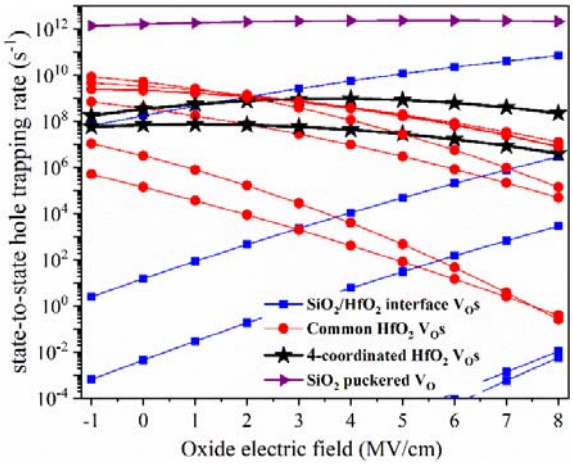

Fig. 18 The electric field dependent hole trapping rate of each defect in the amorphous $Si/SiO_2/HfO_2$ stack.

Finally, we calculate the hole trapping rate of each defect in the $cSi/aSiO_2/aHfO_2$ stack, and their dependence on external electric field. Obviously, there are four kinds of defects in Fig. 18, i.e. the SiO_2/HfO_2 interface V_Os whose hole trapping capability increases monotonically with the electric field, the common HfO_2 V_Os (2- and 3-coordinated) whose hole trapping rates decrease monotonically, the 4-coordinated HfO_2 V_Os whose trapping rate increase first and then decrease after certain field strength, and the puckered SiO_2 V_O defect who is always a strong trapping center due to its closeness to Si in real space and its closeness to VBM_{Si} in energy. In comparison with the results in crystalline $Si/SiO_2/HfO_2$ stacks, two new phenomena need to be pointed out. First, the strong hole trapping rates of puckered V_O defect in SiO_2 overturns the previous

conclusion that VO defects in the SiO_2 part are not effective hole trapping centers compared with those in HfO_2 and interface. Second, although some SiO_2/HfO_2 interface defects are very effective in hole trapping, most of them are not as effective as the defects in HfO_2. In other words, the amorphous $Si/SiO_2/HfO_2$ stack shows us a more complete picture of hole trapping in high-k gate stacks.

IV. CONCLUSIONS

In conclusion, we have proposed an optimized theoretical simulation framework to study the charge trapping across multiple interfaces. By applying this framework to crystalline and amorphous $Si/SiO_2/HfO_2$ stacks, we manage to elucidate the hole trapping mechanism for multiple trapping paths in the structure and identify the dominant hole trapping centers by calculating the exact hole trapping rates under different magnitudes of gate electric field. Results show that the dominant hole trapping centers are neither located at a single material nor limit themselves as a single type. On the contrary, the strong hole trapping center could be a puckered V_O defect or Single-H passivated dimer V_O defect at the SiO_2, some V_O defects at the SiO_2/HfO_2 interface, or most V_O defects inside the bulk HfO_2. Moreover, we find that H passivation is not able to eliminate such hole trapping problem effectively due to the formation of some H-related defects, which are also effective trapping centers. On the contrary, F passivation is found to be more effective in eliminating defect states, and should be paid more attention to. We hope all these conclusions could be instructive in improving the performance of high-k MOSFETs, and the simulation framework could be helpful for studying the charge trapping problems in other semiconductor devices.

Acknowledgement

This work was supported by National Natural Science Foundation of China (grand Nos. 61927901 , 11774338, 11574304), China Key Research and Development Program (2018YFA0306101), Chinese Academy of Sciences-Peking University Pioneer Cooperation Team (CAS-PKU Pioneer Cooperation Team), the Youth Innovation Promotion Association CAS (Grand No. 2016109), and project grand No.6J6011000. Y. Y. Liu acknowledges the support from the National Postdoctoral Program for Innovative Talents (No. BX201700231), and the China Postdoctoral Science Foundation (Grant No. 2018M630194). L. W. Wang was funded by the Joint Center for Artificial Photosynthesis, a DOE Energy Innovation Hub, supported through the Office of Science of the U.S. Department of Energy under Award number DE-SC0004993.

References

[1] L. Larcher, A. Padovani, L. Vandelli, P. Pavan, "Charge transport in high-k stacks for charge-trapping memory applications: A modeling perspective", Microelectronic Engineering 88, 1168-1173 (2011).

[2] C. Zhao, C. Z. Zhao, S. Taylor, and P. R. Chalker, "Review on Non-Volatile Memory with High-k Dielectrics: Flash for Generation Beyond 32 nm", Materials 7, 5117-5145 (2014).

[3] J. H. Stathis and S. Zafar, "The negative bias temperature instability in MOS devices: A review", Microelectron. Reliab. 46, 270–286 (2006).

[4] T. Grasser, et al. "The Paradigm Shift in Understanding the Bias Temperature Instability: From Reaction–Diffusion to Switching Oxide Traps", IEEE Trans. Electron Devices 58, 3652-3666 (2011).

[5] B. H. Lee, et al., "Ultrathin Hafnium Oxide with Low Leakage and Excellent Reliability for Alternative Gate Dielectric Application", in Proceedings of the IEEE International Electron Devices Meeting, 1999, pp. 133-136.

[6] E.P. Gusev, et al., "Ultrathin high-K gate stacks for advanced CMOS devices", in Proceedings of the IEEE International Electron Devices Meeting, 2001, pp. 451-454.

[7] J. Robertson, "High dielectric constant oxides", Eur. Phys. J. Appl. Phys. 28, 265–291 (2004).

[8] C. -L. Kuo and G. S. Hwang, "Structure and Interconversion of Oxygen-Vacancy-Related Defects on Amorphous Silica", Phys. Rev. Lett. 97, 066101 (2006).

[9] N. L. Anderson, R. P. Vedula, P. A. Schultz, R. M. Van Ginhoven, and A. Strachan, "First-Principles Investigation of Low Energy E' Center Precursors in Amorphous Silica", Phys. Rev. Lett. 106, 206402 (2011).

[10] A.-M. El-Sayed, M. B. Watkins, V. V. Afanas'ev, and A. L. Shluger, "Nature of intrinsic and extrinsic electron trapping in SiO_2", Phys. Rev. B 89, 125201 (2014).

[11] A.-M. El-Sayed, M. B. Watkins, T. Grasser, V. V. Afanas'ev, and A. L. Shluger, "Hydrogen-Induced Rupture of Strained Si─O Bonds in Amorphous Silicon Dioxide", Phys. Rev. Lett. 114, 115503 (2015).

[12] A.-M. El-Sayed, Y. Wimmer, W. Goes, T. Grasser, V. V. Afanas'ev, and A. L. Shluger, "Theoretical models of hydrogen-induced defects in amorphous silicon dioxide", Phys. Rev. B 92, 014107 (2015).

[13] E. Mehes and C. H. Patterson, "Defects at the Si(001)/a-SiO_2 interface: Analysis of structures generated with classical force fields and density functional theory", Phys. Rev. Materials 1, 044602 (2017).

[14] F. Cerbu, O. Madia, D. V. Andreev, S. Fadida, M. Eizenberg, L. Breuil, J. G. Lisoni, J. A. Kittl, J. Strand, A. L. Shluger, V. V. Afanas'ev, M. Houssa, and A. Stesmans, "Intrinsic electron traps in atomic-layer deposited HfO_2 insulators", Appl. Phys. Lett. 108, 222901 (2016).

[15] T. Grasser, B. Kaczer, W. Goes, Th. Aichinger, Ph. Hehenberger, M. Nelhiebel, "Understanding negative bias temperature instability in the context of hole trapping", Microelectron. Eng. 86, 1876-1882 (2009).

[16] T. Grasser, B. Kaczer, W. Goes, Th. Aichinger, Ph. Hehenberger, and M. Nelhiebel, "A two stage model for negative bias temperature instability," Proc. Int. Rel. Phys. Symp., 33–44 (2009).

[17] W. Goes, Y. Wimmer, A. -M. El-Sayed, G. Rzepa, M. Jech, A. L. Shluger, T. Grasser, "Identification of oxide defects in semiconductor devices: A systematic approach linking DFT to rate equations and experimental evidence", Microelectron. Reliab. 87, 286-320, 2018.

[18] Y. -Y. Liu, F. Zheng, X. Jiang, J. -W. Luo, S. -S. Li, and L. -W. Wang, "Ab initio investigation of charge trapping across the crystalline-Si/amorphous-SiO_2 interface", Phys. Rev. Appl. 11, 044058 (2019).

[19] A. S. Foster, F. L. Gejo, A. L. Shluger, and R. M. Nieminen, "Vacancy and interstitial defects in hafnia", Phys. Rev. B 65, 174117 (2002).

[20] K. Xiong, J. Robertson, M. C. Gibson, and S. J. Clark, "Defect energy levels in HfO_2 high-dielectric-constant gate oxide", Appl. Phys. Lett. 87, 183505 (2005).

[21] K. Takagi and T. Ono, "First-principles study on leakage current caused by oxygen vacancies at HfO_2/SiO_2/Si interface", Jpn. J. Appl. Phys. 57, 066501 (2018).

[22] E.P. Gusev, C. D_Emic, S. Zafar, A. Kumar, "Charge trapping and detrapping in HfO_2 high-k gate stacks", Microelectron. Eng. 72, 273–277 (2004).

[23] H. W. You and W. J. Cho, "Charge trapping properties of the HfO_2 layer with various thicknesses for charge trap flash memory applications", Appl. Phys. Lett. 96, 093506 (2010).

[24] J. Ji, Y. Qiu, S. Guo, R. Wang, P. Ren, P. Hao, and R. Huang, "New Framework for the Random Charging/Discharging of Oxide Traps in HfO_2 Gate Dielectric: ab-initio Simulation and Experimental Evidence", in Proceedings of the IEEE International Electron Devices Meeting, 2014, pp. 542–545.

[25] K. Tarafder, Y. Surendranath, J. H. Olshansky, A. P. Alivisatos, and L.-W. Wang, "Hole Transfer Dynamics from a CdSe/CdS Quantum Rod to a Tethered Ferrocene Derivative", J. Am. Chem. Soc. 136, 5121−5131 (2014).

[26] Y. -Y. Liu, and X. Jiang, "Physics of hole trapping process in high-k gate stacks: A direct simulation formalism for the whole interface system combining density-functional theory and Marcus theory", in Proceedings of the IEEE International Electron Devices Meeting, 2018, pp. 922–925.

[27] R. A. Marcus, "On the Theory of Oxidation-Reduction Reactions Involving Electron Transfer. I", J. Chem. Phys. 24, 966 (1956).

[28] R. A. Marcus, "On the Theory of Electron-Transfer Reactions. VI. Unified Treatment for Homogeneous and Electrode Reactions", J. Chem. Phys. 43, 679 (1965).

[29] H. Wei, J.-W. Luo, S.-S. Li, and L.-W. Wang, "Revealing the Origin of Fast Electron Transfer in TiO_2-Based Dye-Sensitized Solar Cells", J. Am. Chem. Soc. 138, 8165−8174 (2016).

[30] A. Massé, P. Friederich, F. Symalla, F. Liu, R. Nitsche, R. Coehoorn, W. Wenzel, and P. A. Bobbert, "Ab initio charge-carrier mobility model for amorphous molecular semiconductors", Phys. Rev. B 93, 195209 (2016).

[31] J. Heyd and G. E. Scuseria, “Efficient hybrid density functional calculations in solids: Assessment of the Heyd-Scuseria-Ernzerhof screened Coulomb hybrid functional”, J. Chem. Phys. 121, 1187 (2004).

[32] X. Wang et al., “Band alignment of HfO_2 on SiO_2/Si structure”, Appl. Phys. Lett. 100, 122907 (2012).

[33] Y. Park, K.-j. Kong, H. Chang, and M. Shin, “First-Principles Studies of the Electronic and Dielectric Properties of Si/SiO_2/HfO_2 Interfaces”, Jpn. J. Appl. Phys. 52, 041803 (2013).

[34] E. Nadimi and M. Schreiber, “The influence of lanthanum doping on the band alignment in Si/SiO_2/HfO_2 gate stack of nano-MOSFETs: A first principles investigation”, Phys. Status Solidi B 254, 1700147 (2017).

[35] U. Aschauer and N. A. Spaldin, “Interplay between strain, defect charge state, and functionality in complex oxides”, Appl. Phys. Lett. 109, 031901 (2016).

[36] M. G. Sensoy, D. Vinichenko, W. Chen, C. M. Friend, and E. Kaxiras, “Strain effects on the behavior of isolated and paired sulfur vacancy defects in monolayer MoS_2”, Phys. Rev. B 95, 014106 (2017).

[37] H. Zhu and R. Ramprasad. “Effective work function of metals interfaced with dielectrics: A first-principles study of the Pt-HfO2 interface”, Phys. Rev. B 83, 081416(R) (2011).

[38] https://www.synopsys.com/silicon/quantumatk.html.

[39] J. Schneider, J. Hamaekers, S. T. Chill, S. Smidstrup, J. Bulin, R. Thesen, A. Blom, and K. Stokbro, “ATK-ForceField: a new generation molecular dynamics software package”, Modelling Simul. Mater. Sci. Eng. 25, 085007 (2017).

[40] G. Broglia, G. Ori, L. Larcher, and M. Montorsi. "Molecular dynamics simulation of amorphous HfO_2 for resistive RAM applications", Modelling and Simulation in Materials Science and Engineering 22, 065006 (2014).

[41] E. A. Chagarov and A. C. Kummel, “Ab initio molecular dynamics simulations of properties of a-Al_2O_3/vacuum and a-ZrO_2/vacuum vs a-Al_2O_3/Ge(100)(2×1) and a-ZrO_2/Ge(100)(2×1) interfaces”, J. Chem. Phys. 130, 124717 (2009).

[42] T.-J. Chen and C.-L. Kuo, “First principles study of the structural, electronic, and dielectric properties of amorphous HfO_2”, J. Appl. Phys. 110, 064105 (2011).

[43] P. Broqvist, A. Alkauskas, and A. Pasquarello, “Band alignments and defect levels in Si-HfO_2 gate stacks: Oxygen vacancy and Fermi-level pinning”, Appl. Phys. Lett. 92, 132911 (2008).

[44] G. H. Chen, Z. F. Hou, and X. G. Gong, “Density functional calculations on atomic and electronic structures of amorphous HfO_2/Si(001) interface”, Appl. Phys. Lett. 95, 102905 (2009).

[45] L. C. Gallington, Y, Ghadar, L. B. Skinner, J. K. R. Weber, S. V. Ushakov, A. Navrotsky, A. Vazquez-Mayagoitia, J. C. Neuefeind, M. Stan, J. J. Low, and C. J. Benmore, “The Structure of Liquid and Amorphous Hafnia”, Materials 10, 1290 (2017).

[46] C. Kaneta and T. Yamasaki, “Oxygen-related defects in amorphous HfO_2 gate dielectrics”, Microelectronic Engineering 84 2370-2373 (2007).

[47] W. L. Scopel, A. J. R. da Silva, and A. Fazzio, “Amorphous HfO_2 and $Hf_{1-x}Si_xO$ via a melt-and-quench scheme using ab initio molecular dynamics”, Phys. Rev. B 77, 172101 (2008).

[48] Y. Wang, F. Zahid, J. Wang, and H. Guo, “Structure and dielectric properties of amorphous

high-κ oxides: HfO_2, ZrO_2, and their alloys", Phys. Rev. B 85, 224110 (2012)

[49] W. Jia, Z. Cao, L. Wang, J. Fu, X. Chi, W. Gao, L.-W. Wang, "The analysis of a plane wave pseudopotential density functional theory code on a GPU machine", Comput. Phys. Comm. 184, 9-18 (2013).

[50] W. Jia, J. Fu, Z. Cao, L. Wang, X. Chi, W. Gao, L.-W. Wang, "Fast plane wave density functional theory molecular dynamics calculations on multi-GPU machines", J. Comput. Phys. 251, 102-115 (2013).

[51] F. Zheng, H. H. Pham and L.-W. Wang, "Effects of the c-Si/a-SiO_2 interfacial atomic structure on its band alignment: an ab initio study", Phys. Chem. Chem. Phys. 19, 32617 (2017).

[52] See Supplemental Material at [URL will be inserted by publisher] for the influence of functional (PBE and HSE) on the reorganization energy.

[53] G. L. Closs, L. T. Calcaterra, N. J. Green, K. W. Penfield, and J. R. Miller, "Distance, stereoelectronic Effects, and the Marcus inverted region in intramolecular electron transfer in organic radical anions", J. Phys. Chem. 90, 3673-3683 (1986).

[54] R. J. Carter, E. Cartier, A. Kerber, L. Pantisano, T. Schram, S. De Gendt, and M. Heyns, "Passivation and interface state density of SiO_2/HfO_2-based/polycrystalline-Si gate stacks", Appl. Phys. Lett. 83, 533 (2003).

[55] H. H. Tseng, P. J. Tobin, S. Kalpat, J. K. Schaeffer, M. E. Ramón, L. R. C. Fonseca, Z. X. Jiang, R. I. Hegde, D. H. Triyoso, and S. Semavedam, "Defect Passivation With Fluorine and Interface Engineering for Hf-Based High-k/Metal Gate Stack Device Reliability and Performance Enhancement", IEEE Trans. Electron Devices 54, 3267-3275 (2007).

[56] C. H. Lee, T. Nishimura, T. Tabata, S. K. Wang, K. Nagashio, K. Kita, and A. Toriumi, "Ge MOSFETs Performance: Impact of Ge Interface Passivation", in Proceedings of the IEEE International Electron Devices Meeting, 2010, pp. 416-419.

[57] K. O. Jeppson and C. M. Svensson, "Negative bias stress of MOS devices at high electric fields and degradation of MNOS devices", J. Appl. Phys. 48, 2004 (1977).

[58] L. Tsetseris, X. J. Zhou, D. M. Fleetwood, R. D. Schrimpf, and S. T. Pantelides, "Physical mechanisms of negative-bias temperature instability", Appl. Phys. Lett. 86, 142103 (2005).

[59] T. B. Hook, E. Adler, F. Guarin, J. Lukaitis, N. Rovedo, and K. Schruefer, "The Effects of Fluorine on Parametrics and Reliability in a 0.18-um 3.5/6.8 nm Dual Gate Oxide CMOS Technology", IEEE Trans. Electron Devices 48, 1346-1353 (2007).

[60] K. -i. Seo, R. Sreenivasan, P. C. McIntyre, and K. C. Saraswat, "Improvement in High-k (HfO_2/SiO_2) Reliability by Incorporation of Fluorine", IEEE Electron Device Lett. 27, 821-823 (2006).

[61] Y. Liu, M. R. Halfmoon, C. A. Rittenhouse, and S. Wang, "Passivation effects of fluorine and hydrogen at the SiC-SiO_2 interface", Appl. Phys. Lett. 97, 242111 (2010).

[62] P. Broqvist, A. Alkauskas, J. Godet, and A. Pasquarello, "First principles investigation of defect energy levels at semiconductor-oxide interfaces: Oxygen vacancies and hydrogen interstitials in the Si–SiO_2–HfO_2 stack", J. Appl. Phys. 105, 061603 (2009).

[63] J. K. Rudra and W. B. Fowler, "Oxygen vacancy and the E1' center in crystalline Si02", Phys. Rev. B 35, 8223 (1987).

[64] S. Mukhopadhyay, P. V. Sushko, A. M. Stoneham, and A. L. Shluger, "Modeling of the structure and properties of oxygen vacancies in amorphous silica", Phys. Rev. B 70, 195203

(2004).